ELSEVIER

Cardiovascular Research 51 (2001) 681–690

Cardiovascular Research

www.elsevier.com/locate/cardiores

High resolution optical mapping reveals conduction slowing in connexin43 deficient mice

Benjamin C. Eloff[a], Deborah L. Lerner[b], Kathryn A. Yamada[b], Richard B. Schuessler[b], Jeffrey E. Saffitz[b], David S. Rosenbaum[a,*]

[a]*The Heart and Vascular Research Center and the Department of Biomedical Engineering, MetroHealth Campus, Case Western Reserve University, 2500 MetroHealth Drive, Hamman 322, Cleveland, OH 44109-1998, USA*

[b]*The Departments of Medicine, Pediatrics, Surgery and Pathology, and the Center for Cardiovascular Research, Washington University School of Medicine, St. Louis, MO, USA*

Received 19 January 2001; accepted 24 April 2001

Abstract

Analysis of mice with genetically altered expression of cardiac connexins can provide insights into the role of individual gap junction channel proteins in cell-to-cell communication, impulse propagation, and arrhythmias. However, conflicting results have been reported regarding conduction velocity slowing in mice heterozygous for a null mutation in the gene encoding connexin43 (Cx43). **Methods:** High-resolution optical mapping was used to record action potentials from 256 sites, simultaneously, on the ventricular surface of Langendorff perfused hearts from 15 heterozygous (Cx43+/−) and 8 wildtype (Cx43+/+) mice (controls). A sensitive method for measuring epicardial conduction velocity was developed to minimize confounding influences of subepicardial breakthrough and virtual electrode effects. **Results:** Epicardial conduction velocity was significantly slower (23 to 35%, $P<0.01$) in Cx43+/− mice compared to wildtype. There was no change in conduction patterns or anisotropic ratio (Cx43+/− 1.54±0.33; Cx43+/+ 1.57±0.17) suggesting that Cx43 expression was reduced uniformly throughout myocardium. The magnitude of reductions in conduction velocity and Cx43 protein expression (45%) were similar in mice in which the null allele occurred in a pure C57BL/6J genetic background versus a mixed (C57BL/6J X 129) background. Action potential duration did not differ between mice of different genotypes. **Conclusions:** A ~50% reduction of Cx43 expression causes significant conduction velocity slowing in the Cx43+/− mouse heart. The apparent lack of conduction velocity changes reported in previous studies may be related to technical factors rather than variations in genetic background. High-resolution optical mapping is a powerful tool for investigating molecular determinants of propagation and arrhythmias in genetically engineered mice.

Keywords: Cell communication; Gap junctions; Gene expression; Mapping

This article is referred to in the Editorial by C.A. Eisenberg and L.M. Eisenberg (pages 630–632) in this issue.

1. Introduction

Cardiac gap junction channels are comprised of connexin protein complexes [1,2] which interconnect neighboring myocytes and play a critical role in cell-to-cell communication and conduction. Importantly, the discontinuous nature of conduction in cardiac tissue is attributed to propagation delays at gap junctions [3,4]. Under normal circumstances, junctional propagation delays are roughly equivalent to propagation across the entire myocyte, however, under pathological conditions, the junctional contribution can be considerably greater [5–8]. Consequently, alterations in gap junction protein expression and distribution are thought to play a major role in cardiac pathology. Peters et al. [9] have observed changes in the distribution and arrangement of gap junctions in regions of

*Corresponding author. Tel.: +1-216-778-2005; fax: 1-216-778-4924.
E-mail address: drosenbaum@metrohealth.org (D.S. Rosenbaum).

Time for primary review 18 days

0008-6363/01/$ – see front matter
PII: S0008-6363(01)00341-8

slow conduction which were critical to the development reentrant ventricular tachycardia in healed canine myocardial infarcts. Altered gap junction function has also been associated with changes in AV nodal [10], His Purkinje [11], and atrial [12] conduction. Moreover, there is now evidence that connexins can turn over in the order of 1–2 h [13], potentially allowing rapid synthesis of new gap junction protein in response to various physiological stresses.

Despite their importance in many physiological and pathophysiological situations, it has been difficult to isolate and study the role of gap junctions in animal models of arrhythmias. Drugs which produce uncoupling between isolated myocyte pairs [14,15] also block sodium [16], calcium, and potassium channels [17], alter pH [18], or have effects that do not readily achieve steady-state. The recent advent of transgenic techniques has led to the exciting possibility of genetically altering expression of individual connexins in the intact heart, so as to deduce, with great specificity, the influence of connexins in complex disease models.

Genetically engineered mice lacking the major cardiac gap junction protein, connexin43 (Cx43) have been used to investigate the role of gap junctions in ventricular conduction. Homozygous null animals (Cx43−/−) express no Cx43 and die soon after birth from defects in the right ventricular outflow tract [19]. Recent elegant studies in a conditional Cx43−/− knockout mouse which does not develop outflow tract abnormalities revealed substantial conduction velocity slowing [20]. However, it is likely that human disease is associated with a more subtle depression of Cx43 expression than that seen in Cx43−/− animals. Mice heterozygous for the null mutation (Cx43+/–) exhibit ~50% reduction in Cx43 protein levels compared to wildtype [21], and no apparent compensatory increases in other connexin proteins or upregulation of sodium channel activity [22], making this model well suited for investigating the effect of gap junctions on ventricular conduction and arrhythmias. However, the evaluation of the conduction phenotype of this model has yielded conflicting results. Initial studies involving analysis of ECGs and electrograms recorded from a linear electrode array placed on the ventricular epicardial surface reported slow conduction in isolated perfused Cx43+/− hearts [21,23]. More recently, Morley et al. [24] did not observe significant differences in local conduction or ECG changes in the Cx43+/− mice analyzed by detailed video mapping with voltage sensitive dyes. Because only inbred mice of mixed genetic background (C57BI/6×129) have been studied previously, differences in genetic strain could have contributed to the disparate phenotypes reported in different studies. Consequently, there remains an unresolved question as to whether a nearly 50% reduction in connexin protein content leads to conduction slowing in the intact heart, and if not, why? The major aim of the present investigation was to utilize a newly developed optical mapping system designed specifically for investigating transgenic mice so as to establish the electrophysiological phenotype, if any, in Cx43+/− mice.

2. Methods

2.1. Mouse colonies

Mice of two strains and harboring a Cx43 null mutation were maintained in a standard barrier facility. Founder mice (B6,129-Gja1^{tm1Kdr} or C57BL/6J-Gja1^{tm1Kdr}) were obtained originally from Jackson Laboratory (Bar Harbor, ME). Mice derived from the B6,129 hybrid founders were continuously inbred and are of unknown mixed genetic background. Mice derived from the C57BL/6J founders are congenic. No differences in fertility, litter sizes, genotype distribution, life span or Cx43 expression have been observed between the two groups. The genotypes of all mice were determined by PCR as described previously [22]. The investigation conforms with the *Guide for the Care and Use of Laboratory Animals* published by the US National Institutes of Health.

2.2. Immunoblotting

Western blot analysis was performed on ventricular tissue from adult hearts as previously described [22]. Each lane was loaded with 7 μg of total protein. A control for equal protein loading was performed using an immunoblot for actin which showed similar intensities in all lanes with protein samples from both Cx43+/+ and Cx43+/− animals. Immunoreactivity on blots was detected by chemiluminescence (Rennaissance, NEN Life Science) and quantified by densitometric analysis with Adobe Photoshop.

2.3. Histological analysis of surface fiber orientation

Hearts were excised from Cx43+/− and Cx43+/+ mice, rinsed and fixed in 10% formalin while being gently compressed on glass cover slips to flatten the anterior surface. Paraffin sections were cut from the most superficial regions of the anterior surface (corresponding to the mapped region) and stained with a reticulin stain to highlight the orientation of the surface fibers.

2.4. Mouse langendorff preparation

Mice were anesthetized (0.1 ml Nembutal, 0.1 ml Heparin, i.p.), and hearts were rapidly excised, and rinsed in warm Krebs solution. Hearts were then perfused as Langendorff preparations with warmed (37°C), oxygenated Krebs solution containing (mmol/l): 118.3 NaCl, 4.7 KCl, 1.0 $MgSO_4$, 1.4 KH_2PO_4, 10 Dextrose, 29.0 $NaHCO_3$, 3.4 $CaCl_2$, pH 7.4 [21]. A perfusion pressure of 55 mmHg was

maintained by adjusting flow rates between 1 and 2 ml/min. 10 mmol/l diacetyl monoxime was added to the perfusate to reduce contraction artifacts as described previously [24]. In pilot studies, we found that conduction velocity was unchanged in the presence of diacetyl monoxime. Hearts were continuously perfused with the voltage-sensitive dye, di-4-ANEPPS (4 μmol/l).

For the purpose of monitoring cardiac rhythm, one stainless steel pin (0.1 mm diameter) was inserted into the left atrium, and another into the left ventricle on the posterior basal aspect of the heart. Pseudo-electrocardiograms were recorded from bipolar signals created by this electrode pair. A similar electrode pair was placed on the right atrium and ventricle. A unipolar stimulating electrode (0.05 mm dia.) was positioned on the anterior left ventricular epicardium, 2 mm below the A–V groove and 2 mm lateral to the left anterior descending coronary artery, such that stimuli were delivered to the center of the mapping array (Fig. 1). Hearts were submerged in a specialized recording chamber filled with temperature-controlled (37°C) Krebs buffer that was continuously turned over by coronary effluent. Gentle compression applied to the posterior surface of the heart by a movable piston was used to stabilize the anterior surface of the ventricle against the imaging window to ensure that the entire mapping surface was in focus without altering electrophysiological properties of the preparation [25,26]. The stability of the preparation was assessed by monitoring ECG, diastolic pacing threshold, and perfusion pressure throughout the experiment. Adequacy of perfusion and tissue viability was further accessed by microscopic examination of each heart following staining with 2,3,5-triphenyltetrazolium chloride. Hearts used in these studies exhibited no evidence of instability and remained viable for at least 3 h of perfusion, while the experimental protocols were typically completed within 45 min. Also, pilot studies revealed no significant tissue edema during the time period required to perform these experiments (baseline heart weight 182±29 mg, final heart weight 183±34 mg, $n=7$).

2.5. High resolution optical mapping system

Optical action potentials were recorded simultaneously from 256 sites on the anterior surface of the ventricle (Fig. 1). Fluorescence was excited with a 270 Watt tungsten halogen light (filtered 500±25 nm). The quality of action potentials recorded under high magnification were optimized by a tandem-lens imaging system [27]. The tandem-lens system is a pair of single-lens-reflex photographic lenses (35 mm, f/1.4; 105 mm, f/2, Nikon Corporation), focused at infinity, and placed with the bayonet mounts facing outwards. (Fig. 2) The tissue preparation is placed in the focal plane of the objective lens, and a 16×16 photodiode array (C4675-102, Hammamatsu Corporation) is placed at the focal plane of the detector lens. Fluorescent light exiting the detector lens is passed through an emission filter (>610 nm) before being focused onto the photodiode array. By inserting a removable mirror behind the objective lens, an image of the heart was projected onto a CCD video camera allowing direct visualization of cardiac anatomy in relation to the action potential mapping field (Fig. 2). Optical magnification, which is determined by the ratio of focal lengths of the detector lens to the objective lens was 3×, providing 367 μm resolution between recording pixels.

Photocurrent from each photodiode underwent current-to-voltage conversion, amplification (200×), bandpass filtering (0.1–1500 Hz), and was multiplexed and digitized (3400 samples/s/channel) with 12-bit precision. In preliminary studies we found that this sampling rate was adequate for reconstructing the high frequency components of optically recorded mouse action potentials which was typically under 1500 Hz. Action potentials recorded with this system depicted the time course of membrane potential change with fidelity comparable to action potentials recorded with microelectrodes [28].

2.6. Experimental protocol

The electrophysiological properties of the Cx43+/− mice ($n=15$) were compared to wildtype (Cx43+/+) controls ($n=8$). Additional analyses were performed comparing electrophysiological properties of the subset of Cx43+/− and Cx43+/+ mice bred in congenic (Cx43+/−, $n=10$; Cx43+/+, $n=5$) and mixed (Cx43+/−, $n=5$; Cx43+/+, $n=3$) genetic backgrounds. Constant cycle length (CL) stimulation was performed at CLs of 170 to 100 ms, by 10 ms decrements, with a stimulus current just above (within 0.2 mA) diastolic threshold, and a pulse width of 0.5 ms. Action potentials were recorded during steady-state (>1 min) pacing at each CL for 5 s. Investigators performing experiments and data analysis were blinded to the genotype of each animal. Genotype was determined by one investigator who was blinded to the outcome of the experiments.

2.7. Data analysis

Data analysis was performed using custom software designed specifically for the analysis of action potentials recorded optically from the mouse heart. The point of maximum upstroke slope of each action potential was taken as local depolarization time as described previously [30]. Action potential duration was defined as the time interval between depolarization and 70% return of repolarization to resting potential (APD_{70}). Action potential upstroke rise time was measured from the time interval between the first two zero crossings of the first derivative of the action potential upstroke. This corresponded to the time from initial depolarization from resting potential to the termination of the upstroke. Because the optically

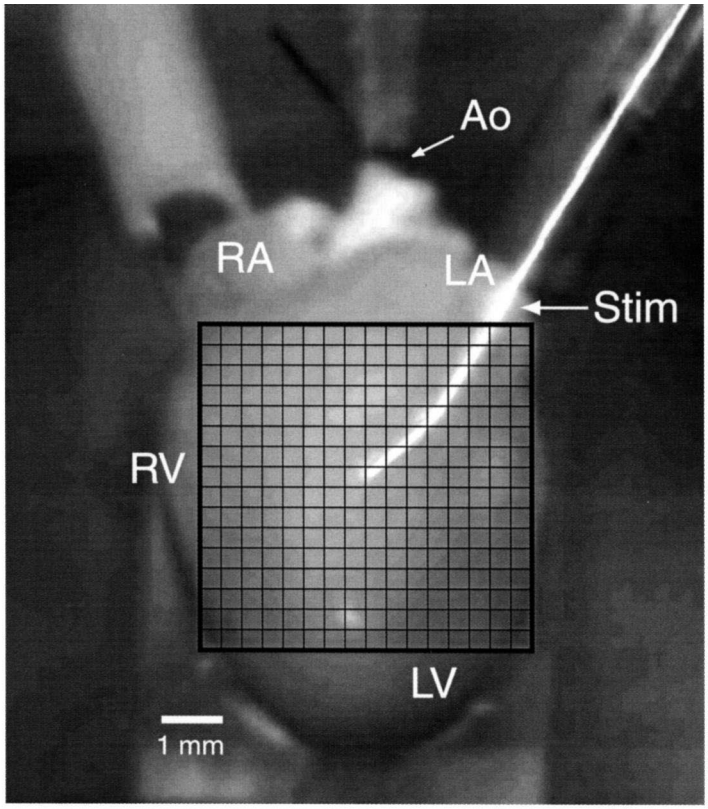

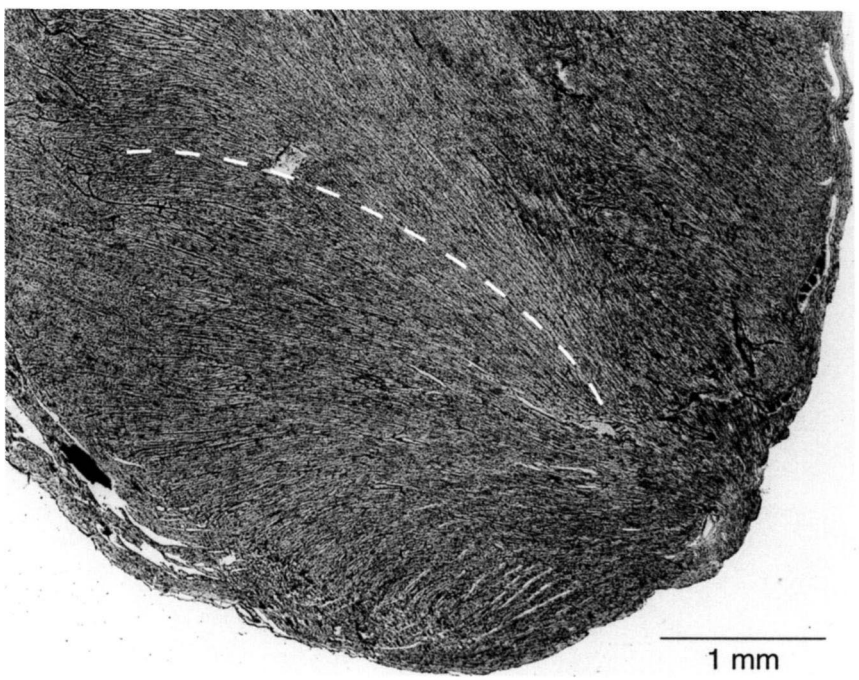

Fig. 1. Optical action potentials recorded from 256 sites in a 5.8×5.8 mm mapping area (square grid, top). The left ventricle was stimulated from the center of the mapping field. Histological section of the anterior surface of a mouse heart (bottom). The image corresponds approximately to the mapping area illustrated above. The section has been stained with a reticulin stain to highlight the orientation of surface fibers. The directions of fast and slow conduction shown in the contour plots in Fig. 6 correspond well with longitudinal (dashed line) and transverse surface fiber orientations, respectively. Original magnification: 20×. RA: right atrium; LA: left atrium; RV: right ventricle; LV: left ventricle; Ao: aorta; Stim: stimulus electrode.

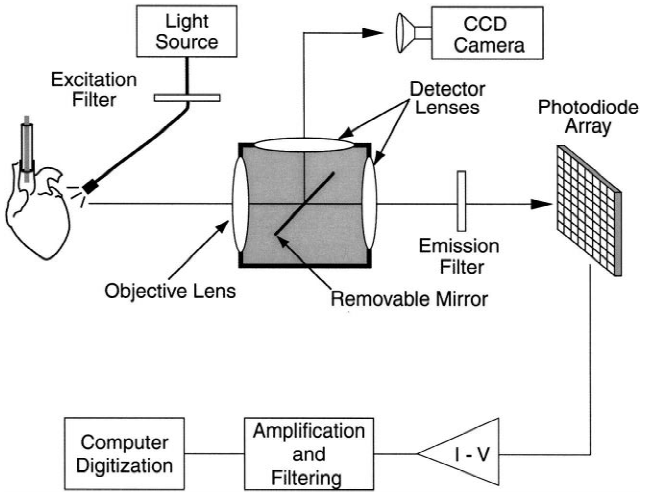

Fig. 2. High-resolution optical mapping system. Optical mapping was performed by exciting voltage-sensitive dye bound to myocytes of intact hearts using filtered (500±25 nm) light from tungsten halogen source. Voltage-dependent fluoresced light was then collected by the objective lens and transmitted through a light-tight box to a detector lens. The detector lens was selected by adding or removing a mirror from the box. Light exiting the detector lens was focused directly onto the CCD camera, or through an emission filter (>610 nm) onto the 16×16 photodiode array. Current produced by the photodiode array underwent current-to-voltage conversion and the signal was passed through a gain and filtering stage into a multiplexer and 12-bit analog-to-digital converter for computer digitization.

recorded action potential arises from a small aggregate of cells, the upstroke can be blurred by propagation between cells located within an optical pixel. Previously, we developed a method which compensates for blurring artifact and produces a corrected rise time which is comparable to the rise time measured from single cells with microelectrodes [25].

The technique of Bayly et al. [31] was modified for the purpose of calculating conduction velocity in the intact mouse heart. Velocity vectors, which represent the magnitude and direction of conduction velocity at each recording site, were calculated by fitting the depolarization time measured at each site to a parabolic surface, and assigning the gradient of this surface as the velocity vector. Conduction velocities were averaged across sites located within 660 μm of the line that defined each conduction path. Average velocities were calculated for conduction paths spreading from the central stimulus site for every 30° (0–360°). The lines of conduction having the two maximum and two minimum conduction velocities, corresponding with conduction longitudinal and transverse to cardiac fibers are reported in this study. To eliminate artifactual increases in conduction velocity due to local simultaneous capture of multiple pixels proximal to the stimulus site (i.e. virtual electrode effect), or errors in conduction velocity caused by subepicardial breakthrough distal to the stimulus site, outlier vectors were eliminated prior to averaging if they met either of the following criteria: velocity vectors along any given propagation angle deviated more than 15° from the propagation angle under consideration; any individual velocity vector magnitude deviated from the mean magnitude by more than 2 standard deviations. These criteria were defined prospectively and applied uniformly to analysis of conduction velocity in all experiments.

2.8. Statistical analysis

Comparisons of mean conduction velocities were made using Student's *t*-test with Bonforoni correction where appropriate. Comparisons of repeated measurements of conduction velocity at different pacing cycle lengths were made using two-way ANOVA. All values are reported as mean±standard deviation. A $P<0.05$ was considered significant.

3. Results

3.1. Cx43 protein expression

Previous studies of Cx43 expression levels in Cx43+/– mice have involved animals of mixed genetic background only. To determine whether a similar reduction in Cx43 expression occurs in congenic mice, Western blot analysis was performed on ventricular tissue homogenates of 8 hearts (4 Cx43+/+, 4 Cx43+/−) from congenic mice. Fig. 3 shows a representative immunoblot. Quantitative densitometric analysis revealed that Cx43 protein expres-

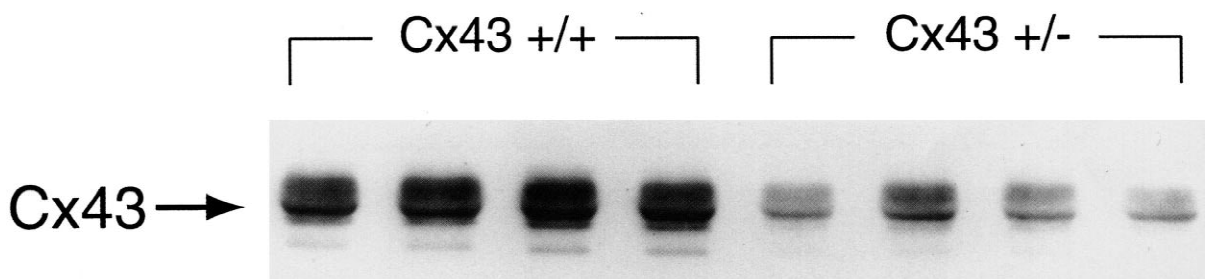

Fig. 3. Immunoblot demonstrating ~50% reduction in Cx43 protein expression in Cx43+/− versus Cx43+/+ hearts from congenic C57BL/6J mice. Equal amounts of protein (7 μg) were loaded into each lane of the gel.

sion in congenic Cx43+/− hearts was reduced by 45% of Cx43+/+ (densities of 0.95±0.05 and 0.52±0.10, respectively). These data corroborate previous reports of reduced Cx43 protein expression in Cx43-deficient mice of a mixed genetic background [21,23] and confirm that Cx43 expression is reduced by ~50% in mice from either mixed or congenic colonies.

3.2. Fiber orientation

Examination of reticulin-stained sections revealed a consistent pattern in which superficial fibers swept across the anterior surface from right to left and base to apex as illustrated in a representative image (Fig. 1, bottom). No apparent differences in fiber orientation were observed in Cx43+/+ (n=6) and Cx43+/− (n=6) hearts.

3.3. Action potential parameters

Representative examples of ECG's and action potentials recorded from Cx43+/− and Cx43+/+ hearts are shown in Fig. 4. Although the onset of the ECG QRS complex coincided with each optical action potential upstroke, the timing of repolarization was much more difficult to discern from the ECG's than the action potentials, and it was not possible to differentiate the terminal portion of the QRS complex from the T-wave on the ECG [29]. APD_{70} measured in all hearts during steady state pacing (CL=140 ms) did not differ significantly between Cx43+/− (19.0±3.6 ms) and Cx43+/+ hearts (20.9±3.4 ms), nor were there any clear differences in the overall morphology of action potentials recorded from mice of each genotype. Action potential upstroke rise time was compared between Cx43+/− and Cx43+/+ mice for cells located along the fast and slow axes of propagation. As shown in Fig. 5, corrected rise time was significantly ($P<0.01$) faster during conduction transverse compared to conduction longitudinal to fibers, consistent with a mechanism of conduction slowing related to increased axial resistivity rather than depressed excitability. Similarly, although there was no difference in raw rise time, corrected rise time was faster in Cx43+/− compared to Cx43+/+ mice during conduction transverse to fibers, implicating a mechanism of conduction slowing in Cx43+/− mice consistent with altered gap junction expression.

3.4. Conduction velocity

Representative conduction maps are shown in Fig. 6. The pattern of anisotropic spread of activation from the point of stimulation was similar in Cx43+/− and Cx43+/+ mice (Fig. 6). Relative crowding of isochrone lines in the Cx43+/− heart (left panel) indicates conduction slowing when compared to the Cx43+/+ heart (right panel). In both examples there was a relatively large initial isochrone caused by local simultaneous capture of multiple sites in proximity to the stimulus electrode. This led to an apparent rather than actual increase in local conduction

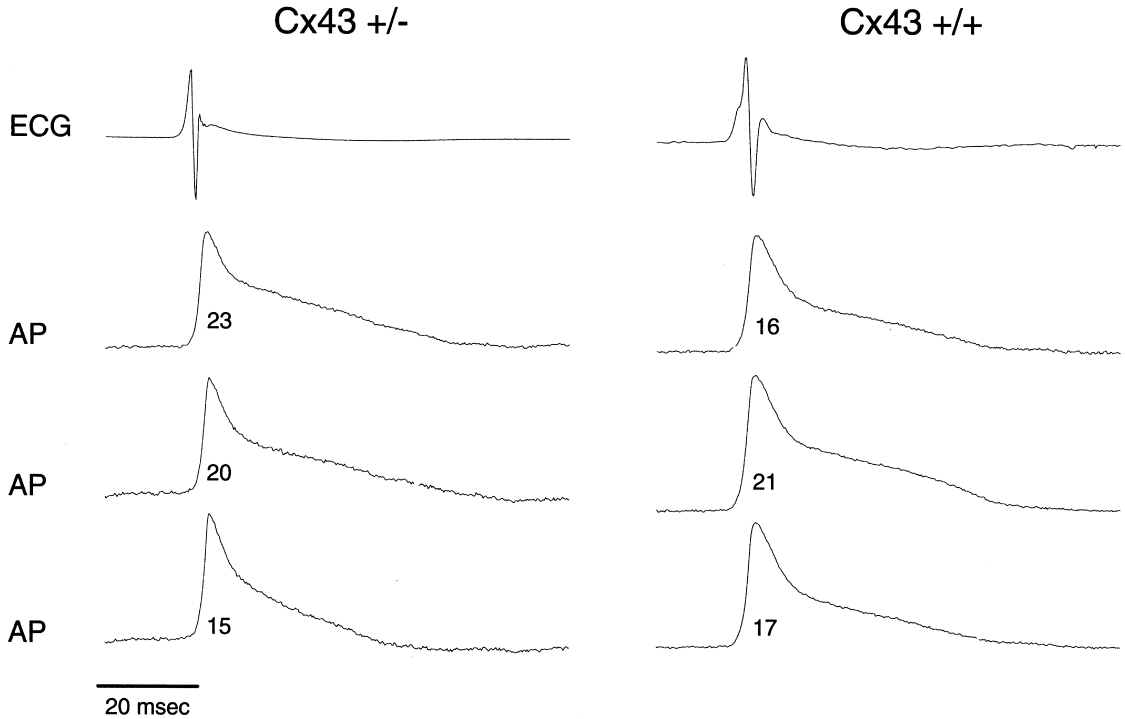

Fig. 4. Electrocardiogram (ECG) and optical action potentials (AP) recorded from three representative sites on the epicardial surface of the mouse ventricle. Optical action potentials delineated the time course of membrane potential changes in mouse ventricle with high signal fidelity. APD_{70} was calculated for each action potential shown. Note the ambiguity in identifying the time course of repolarization from the ECG as compared to the AP.

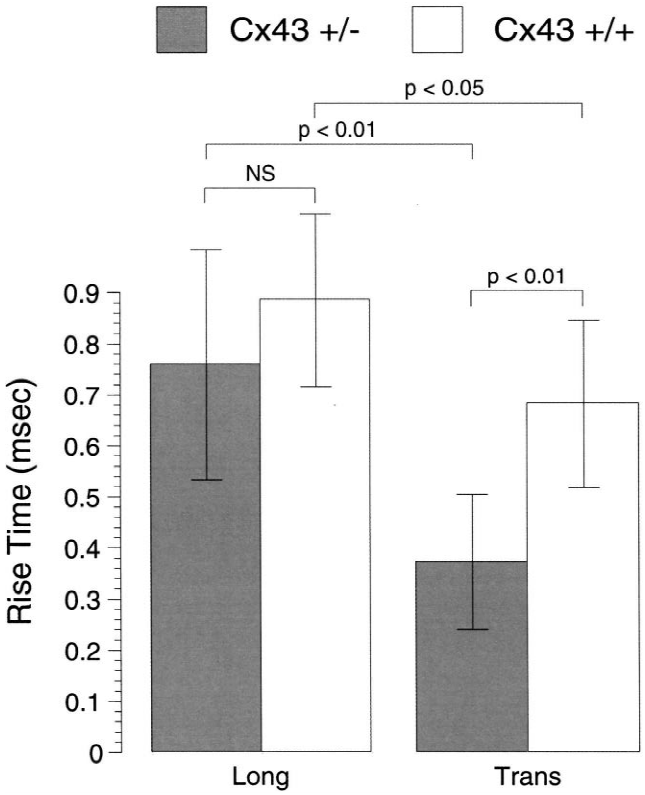

Fig. 5. Corrected action potential rise time for propagation longitudinal (long) and transverse (trans) to fibers. Average values calculated for mice bred from congenic background (n=15). Note that corrected rise times are reduced during propagation transverse compared to longitudinal to fibers, consistent with increased axial resistance in the transverse direction. Corrected rise time is increased in Cx43+/− mice compared to Cx43+/+ mice, although this increase achieved statistical significance only for propagation transverse to fibers.

velocity, and the algorithm used to calculate conduction velocity appropriately discarded vectors in this region (black vectors). The white arrows shown in Fig. 6 represent the vectors used in the calculation of mean conduction velocity for conduction along the fastest and slowest propagation pathways. The orientations of these pathways correspond well with our findings of the longitudinal (fast) and transverse (slow) axes of epicardial ventricular fibers. When considering all experiments (Fig. 7, left panel), conduction velocity was significantly ($P<0.01$, unpaired t-test) slower in Cx43+/− than Cx43+/+ mice.

To assess the effect of genetic background on conduction parameters, hearts from mice of both congenic and mixed backgrounds were compared separately at a CL of 140 ms. Fig. 7 shows that conduction was significantly slowed transverse to fibers for Cx43+/− mice of the mixed and congenic backgrounds. There was also slowing in the longitudinal direction in Cx43+/− mice from both groups, although the mixed group did not achieve significance due to the relatively small sample size. This result argues against the presence of heterogeneous genetic modifiers of the conduction phenotype.

Conduction velocities and anisotropic conduction velocity ratios were compared across a range of CL's. The Cx43+/− hearts exhibited significantly slower velocities at all CL's in both longitudinal (Fig. 8, top) and transverse (Fig. 8, center panel) directions relative to fiber orientation. The magnitudes of the difference in conduction velocity between Cx43+/− and control mice were constant across CL's. There was a slight reduction in conduction velocity at faster CL's, which corresponds well with conduction velocity to CL relationships reported previously [32]. This relationship was present across genotype and fiber orientation. The pattern of conduction spread, and anisotropic ratio did not differ between Cx43+/− (1.53±0.40) and Cx43+/+ (1.59±0.15) hearts (Fig. 8, bottom panel).

4. Discussion

The principal finding of this report is that a 50% reduction in expression of the major cardiac gap junction protein Cx43 leads to significant slowing of conduction velocity in the intact ventricle. Previously, it was difficult to ascertain the effect of altered gap junction expression and function at the level of the intact heart. The finding of this study suggest that the application of voltage-sensitive dye mapping to the Cx43+/− mouse can potentially provide an important tool for investigating the role of connexins in propagation and susceptibility to arrhythmias.

We found that ~50% reduction of Cx43 expression caused significant reductions in conduction velocity in directions both longitudinal and transverse to fiber orientation. This finding is consistent with previous studies of Cx43+/− mice which have shown reduction in the number of gap junctions between neighboring myocytes but no changes in mean gap junction size [33], compensatory changes in Cx40 or Cx45 expression [23], or suppression of membrane currents [22]. The preservation of normal conduction patterns and anisotropic ratio in the Cx43+/− mouse suggests that Cx43 expression was reduced uniformly throughout the myocardium. The fact that despite having slower conduction velocity, action potential rise time is shorter in Cx43+/− mice supports a mechanism of conduction slowing caused by intercellular uncoupling rather than depressed excitability [3]. Moreover, the extent of conduction slowing seen in Cx43+/− hearts (about 25%) is consistent with theoretical predictions where conduction velocity varies as the square root of axial conductance [34]. Therefore, if one assumes that a 50% reduction of Cx43 protein corresponds to a 50% reduction in axial conductance, a 30% reduction in conduction velocity, as observed in these experiments, is expected.

Previously, Guerrero et al. [21] and Thomas et al. [23] used a linear array of extracellular electrodes to record significant conduction slowing in Cx43+/− hearts com-

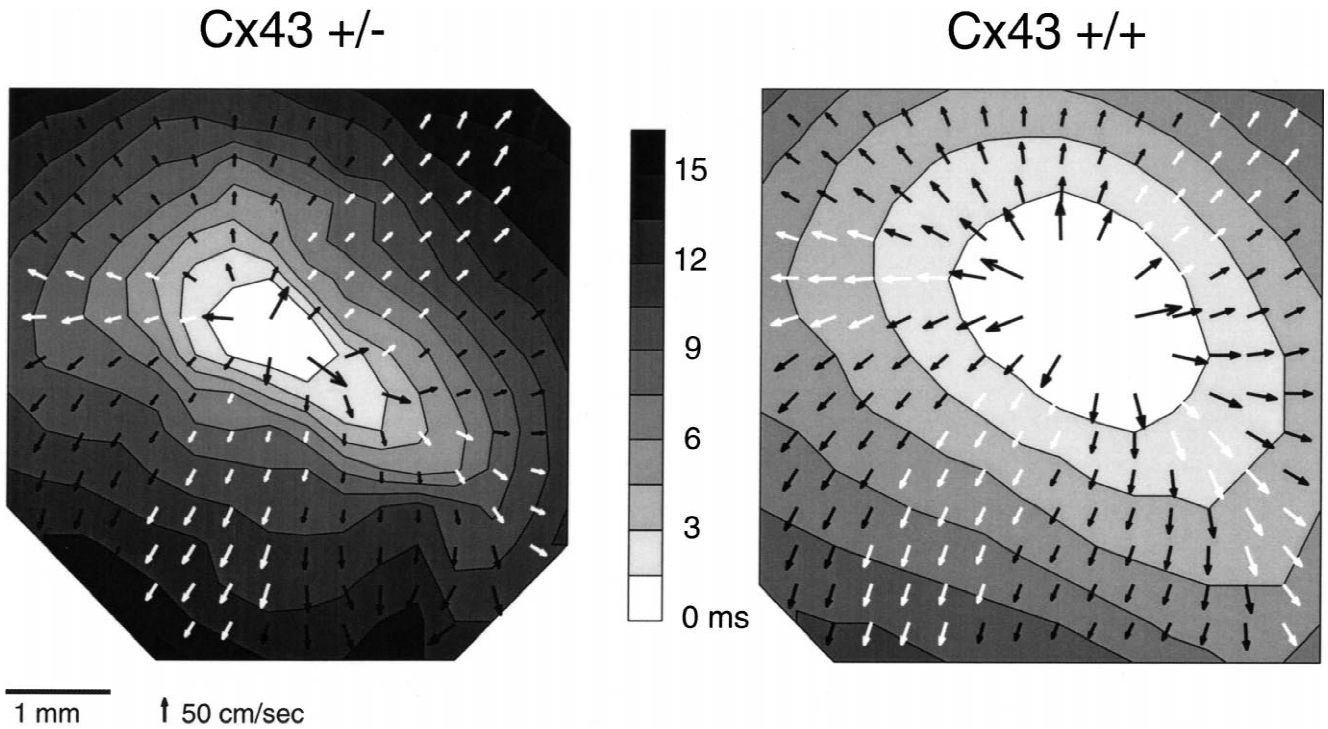

Fig. 6. Contour plots (1.5 ms isochrone lines) demonstrating the sequence and pattern of propagation from the point of stimulation in a representative Cx43+/− heterozygous (left) and Cx3+/+ wildtype (control) counterpart shown to the right. In each case, the impulse spreads anisotropically according to fiber orientation. Although the patterns of conduction are similar, the Cx43+/− heart is associated with substantially slower conduction velocity (crowding of isochrones). Method used to calculate conduction velocity was based on calculation of local velocity vectors (arrows) at each recording site. A computer algorithm was used to group vectors along any selected line of propagation. Shown in this example are vectors selected for propagation along lines of conduction longitudinal and transverse to fibers (white arrows), in addition to vectors determined to fall outside these lines (black arrows) by the algorithm. Conduction velocity along any path was calculated from the average of all vectors selected along a given conduction path.

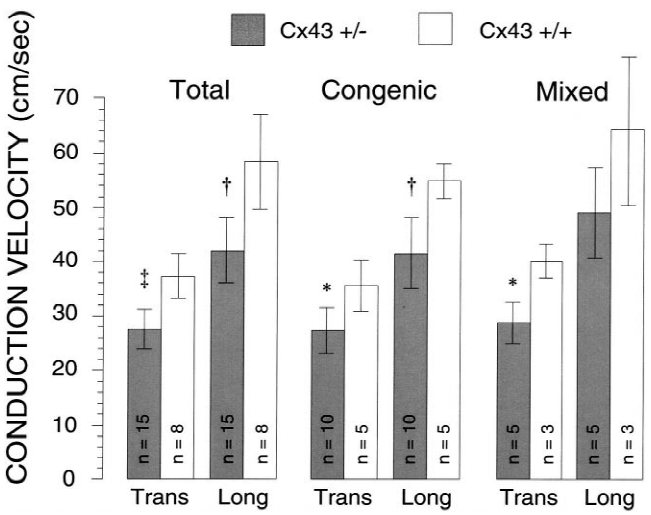

Fig. 7. Conduction velocity measured along the slow and fast fiber axis in Cx43+/− (n=15) vs. Cx43+/+ (n=8) mice at a pacing CL of 140 ms. Conduction velocity was significantly reduced in the Cx43+/− mice when results from congenic and mixed genetic backgrounds groups were combined (left). Similar results were observed when subsets of congenic (Cx43+/−, n=10; Cx43+/+, n=5, center) or mixed genetic background (Cx43+/−, n=5; Cx43+/+, n=3, right) mice were analyzed separately. Significance levels shown for Cx43+/− relative to Cx43+/+ Long: Longitudinal axis; Trans: Transverse axis; *: $P<0.05$; †: $P<0.01$; ‡: $P<0.005$.

pared with wild-type controls. The magnitudes of the change in conduction velocity reported previously [21,23] are larger than those observed in the present study and are likely due to differences in experimental methods and protocols including the use of cold cardioplegia in the earlier studies [21,23]. The values obtained in the present study are probably more indicative of the true conduction phenotype in these mice, due not only to improved experimental procedures, but also to use of voltage-sensitive dye techniques which permit mapping of activation sequences with much greater spatial resolution and identification of local depolarizations directly from multi-site action potentials.

More recently, Morley et al. [24] used voltage-sensitive dyes and video camera imaging in an elaborate study designed to further characterize conduction in Cx43-deficient mice. The ventricular conduction patterns and mean conduction velocities obtained in Cx43+/− mice in the present study are remarkably similar to those reported by Morley et al., [24] and serve not only to corroborate the previous findings, but also to demonstrate the reproducibility of optical mapping procedures using two independent systems. In contrast Morley et al., we report significant conduction velocity slowing in Cx43 deficient mice, perhaps by virtue of the greater temporal and voltage

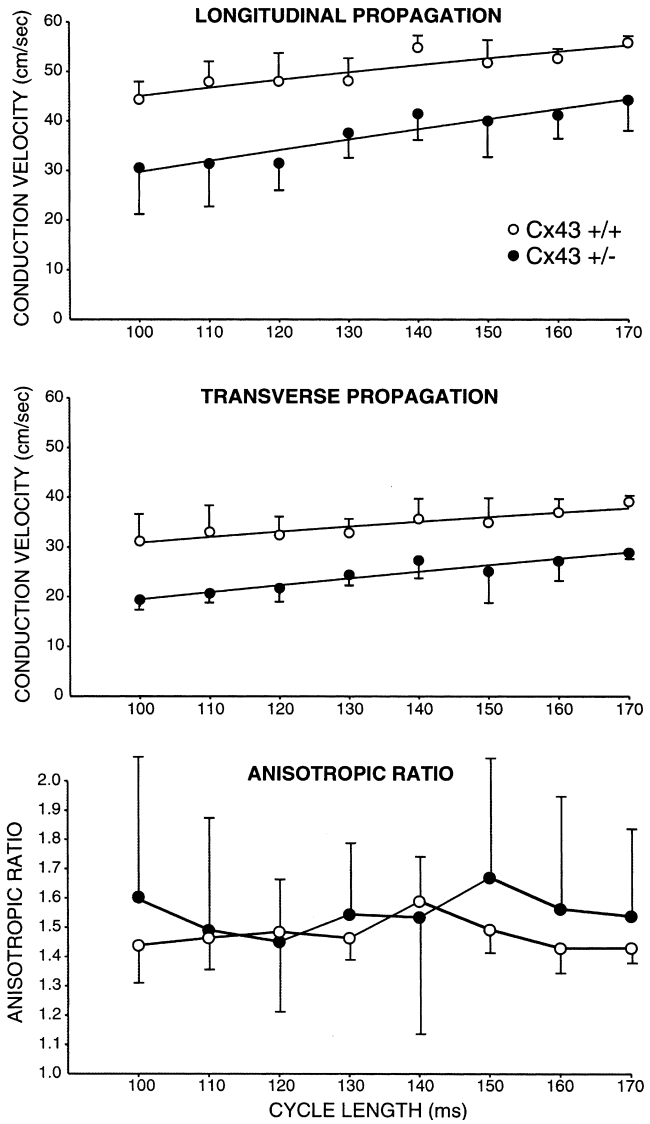

Fig. 8. Cycle length dependence of conduction velocity in congenic Cx43+/− mice. Conduction velocity was considerably slower in Cx43+/− mice along fast and slow axes of propagation. As expected, conduction velocity was slower at more rapid cycle lengths. However, conduction velocity in the Cx43+/− mouse was always slower at all cycle lengths tested. The ratio of fast axis to slow axis conduction velocity (anisotropic ratio) did not differ between Cx43+/− and Cx43+/+ mice at all cycle lengths tested.

resolutions inherent in using tandem-lens imaging and a photodiode array for optical mapping. For instance, the 30% reduction in conduction velocity we observed in Cx43+/− mice were associated with conduction delays of only 6 ms across the entire mapping field, and 0.38 ms between neighboring recording sites. Although readily measurable with the photodiode array sampling interval of 0.29 ms used in our study, such differences would be difficult to detect using video camera sampling rates (4–33 ms) [24,35]. In addition, we used unipolar stimulation with minimal current strength and duration and compensated for the virtual electrode effect [36,37] in our analysis algorithm to determine sites depolarized by propagating wavefronts rather than by direct stimulation. These combined procedures likely contributed to delineation of the significant difference in conduction velocities between Cx43+/− and Cx43+/+ hearts in the present study.

The present study also points out several limitations of investigating electrophysiological phenotypes in mice from the surface ECG. It was not possible for us to distinguish the terminal portion of the QRS complex from the T wave, Others have reported this difficulty as well [29]. In addition, the time course of repolarization was relatively ambiguous on the ECG compared to its clear delineation in optical action potential tracings (Fig. 4). Thus, in the Cx43-deficient mouse in which the major phenotype is modest slowing of conduction, the ECG (i.e. QRS duration) is not a particularly sensitive analytical tool. Direct measurements of conduction are required to define the phenotype. However, in other mouse models or under pathophysiological conditions the ECG may be useful in defining phenotypes. For example, in circumstances associated with pronounced alterations of ventricular conduction such as in bundle branch block, it is easier to detect abnormalities on the mouse ECG [38].

The results of this study provide direct evidence that a ~50% reduction in Cx43 protein expression leads to significant conduction velocity slowing in the intact heart. This was shown to be true for reduced Cx43 expression in two different strains of inbred mice. High-resolution optical mapping is a powerful technique to investigate the role of gap junctions in cardiac propagation, cell-to-cell communication, and arrhythmias. Although the difference in conduction velocity between Cx43+/− and Cx43+/+ mice is modest, when combined with other structural or metabolic derangements present in the diseased heart, this conduction phenotype is likely to manifest itself as an arrhythmogenic substrate [39].

Acknowledgements

The authors thank Evelyn Kanter, for technical assistance with immunoblotting experiments, and Michael Koo, for assistance in data analysis. This study was supported by National Institutes of Health grants HL-54807 and HL-58597, the Medical Research Service of the Department of Veterans Affairs, and the American Heart Association.

References

[1] Perkins GP, Goodenough D, Sosinsky G. Three-dimensional structure of the gap junction connexon. Biophys J 1997;72:533–544.
[2] Spray DC, Harris AL, Bennet MVL. Gap junctional conductance is a simple and sensitive function of intracellular pH. Science 1981;211:712–715.
[3] Spach MS, Miller W, Geselowitz D, Barr R, Kootsey J, Johnson E.

The discontinuous nature of propagation in normal canine cardiac muscle. Circ Res 1981;48:39–54.
[4] Spach MS, Dolber PC. The relation between discontinuous propagation in anisotropic cardiac muscle and the 'vulnerable period' of reentry. In: Zipes DP, Jalife J, editors, Cardiac electrophysiology and arrhythmias, Orlando: Grune & Stratton, 1985, pp. 241–251.
[5] Quan W, Rudy Y. Unidirectional block and reentry of cardiac excitation: A model study. Circ Res 1990;66:367–382.
[6] Shaw RM, Rudy Y. Ionic mechanisms of propagation in cardiac tissue — Roles of the sodium and L-type calcium currents during reduced excitability and decreased gap junction coupling. Circ Res 1997;81:727–741.
[7] Rohr S, Kucera JP, Kléber AG. Slow conduction in cardiac tissue. I: Effects of a reduction of excitability versus a reduction of electrical coupling on microconduction. Circ Res 1998;83:781–794.
[8] Kucera JP, Kléber AG, Rohr S. Slow conduction in cardiac tissue. II: Effects of branching tissue geometry. Circ Res 1998;83:795–805.
[9] Peters NS, Severs NJ, Rothery SM, Lincoln C, Yacoub MH, Green CR. Spatiotemporal relation between gap junctions and fascia adherens junctions during postnatal development of human ventricular myocardium. Circulation 1994;90:713–725.
[10] Simon AM, Goodenough DA, Paul DL. Mice lacking connexin40 have cardiac conduction abnormalities characteristic of atrioventricular block and bundle branch block. Curr Biol 1998;8:295–298.
[11] Jalife J, Sicouri S, Delmar M, Michaels DC. Electrical uncoupling and impulse propagation in isolated sheep purkinje fibers. Am J Physiol 1989;257:H179–H189.
[12] Kirchhoff S, Nelles E, Hagendorff A, Krüger O, Traub O, Willecke K. Reduced cardiac conduction velocity and predisposition to arrhythmias in connexin40-deficient mice. Curr Biol 1998;8:299–302.
[13] Beardslee MA, Laing JG, Beyer EC, Saffitz JE. Rapid turnover of connexin43 in the adult rat heart. Circ Res 1998;83:629–635.
[14] Bastiaanse EML, Jongsma HJ, Van der Laarse A, Takens-Kwak BR. Heptanol-induced decrease in cardiac gap junctional conductance is mediated by a decrease in the fluidity of membranous cholesterol-rich domains. J Membr Biol 1993;136:135–145.
[15] Cole WC, Picone JB, Sperelakis N. Gap junction uncoupling and discontinuous propagation in the heart. A comparison of experimental data with computer simulations. Biophys J 1988;53:809–818.
[16] Nelson WL, Makielski JC. Block of sodium current by heptanol in voltage-clamped canine cardiac Purkinje cells. Circ Res 1991;68:977–983.
[17] Takens-Kwak BR, Jongsma HJ, Rook MB, Van Ginneken AC. Mechanims of heptanol-induced uncoupling of cardiac gap junctions: a perforated patch-clamp study. Am J Physiol 1992;262:C1531–C1538.
[18] Pappas CA, Rioult MG, Ransom BR. Octanol, a gap junction uncoupling agent, changes intracellular [H+] in rat astrocytes. Glia 1996;16:7–15.
[19] Reaume AG, de Sousa PA, Kulkarni S et al. Cardiac malformation in neonatal mice lacking connexin43. Science 1995;267:1831–1834.
[20] Gutstein DE, Morley GE, Tamaddon H et al. Conduction slowing and sudden arrhythmic death in mice with cardiac-restricted inactivation of connexin43. Circ Res 2001;88(3):333–339.
[21] Guerrero PA, Schuessler RB, Davis LM et al. Slow ventricular conduction in mice heterozygous for a connexin43 null mutation. J Clin Invest 1997;99:1991–1998.
[22] Johnson CM, Green KG, Kanter EM, Bou-Abboud E, Saffitz JE, Yamada KA. Voltage-gated Na^+ channel activity and connexin expression in Cx43-deficient cardiac myocytes. J Cardiovasc Electrophysiol 1999;10:1390–1401.
[23] Thomas SA, Schuessler RB, Berul CI et al. Disparate effects of deficient expression of connexin43 on atrial and ventricular conduction — Evidence for chamber-specific molecular determinants of conduction. Circulation 1998;97:686–691.
[24] Morley GE, Vaidya D, Samie FH, Lo C, Delmar M, Jalife J. Characterization of conduction in the ventricles of normal and heterozygous Cx43 knockout mice using optical mapping. J Cardiovasc Electrophysiol 1999;10:1361–1375.
[25] Girouard SD, Laurita KR, Rosenbaum DS. Unique properties of cardiac action potentials recorded with voltage-sensitive dyes. J Cardiovasc Electrophysiol 1996;7:1024–1038.
[26] Laurita KR, Girouard SD, Rosenbaum DS. Modulation of ventricular repolarization by a premature stimulus: Role of epicardial dispersion of repolarization kinetics demonstrated by optical mapping of the intact guinea pig heart. Circ Res 1996;79:493–503.
[27] Ratzlaff EH, Grinvald A. A tandem-lens epifluorescence macroscope: hundred-fold brightness advantage for wide-field imaging. J Neurosci Methods 1991;36:127–137.
[28] Zhou J, Jeron A, London B, Han XQ, Koren G. Characterization of a slowly inactivating outward current in adult mouse ventricular myocytes. Circ Res 1998;83:806–814.
[29] Goldbarg AN, Hellerstein HK, Bruell JH, Daroczy AF. Electrocardiogram of the normal mouse, mus musculus: General considerations and genetic aspects. Cardiovasc Res 1968;2:93–99.
[30] Girouard SD, Pastore JM, Laurita KR, Gregory KW, Rosenbaum DS. Optical mapping in a new guinea pig model of ventricular tachycardia reveals mechanisms for multiple wavelengths in a single reentrant circuit. Circulation 1996;93:603–613.
[31] Bayly PV, KenKnight BH, Rogers JM, Hillsley RE, Ideker RE, Smith WM. Estimation of conduction velocity vector fields from epicardial mapping data. IEEE Trans Biomed Eng 1998;45:563–571.
[32] Boyett MR, Jewell BR. Analysis of the effects of changes in rate and rhythm upon electrical activity in the heart. Prog Biophys Mol Biol 1980;36:1–52.
[33] Saffitz JE, Green KG, Kraft WJ, Schechtman KB, Yamada KA. Effects of diminished expression of connexin43 on gap junction number and size in ventricular myocardium. Am J Physiol Heart Circ Physiol 2000;278:H1662–H1670.
[34] Rudy Y, Quan W. A model study of the effects of the discrete cellular structure on electrical propagation in cardiac tissue. Circ Res 1987;61:815–823.
[35] Baxter WT, Davidenko JM, Loew LM, Wuskell JP, Jalife J. Technical features of a C.C.D. video camera system to record cardiac fluorescence data. Ann Biomed Eng 1997;25:713–725, Jul–Aug.
[36] Lindemans FW, Denier van der Gon JJ. Current thresholds and liminal size in excitations of heart muscle. Cardiovasc Res 1978;12:477–485.
[37] Lindemans FW, Zimmerman AN. Acute voltage, charge, and energy thresholds as functions of electrode size for electrical stimulation of the canine heart. Cardiovasc Res 1979;13:383–391.
[38] Jalife J, Morley GE, Vaidya D. Connexins and impulse propagation in the mouse heart. J Cardiovasc Electrophysiol 1999;10:1649–1663.
[39] Lerner DL, Yamada KA, Schuessler RB, Saffitz JE. Accelerated onset and increased incidence of ventricular arrhythmias induced by ischemia in Cx43-deficient mice. Circulation 2000;101:547–552.